

Measurement of the B^+ and B^0 Lifetimes from Semileptonic Decays at SLD**

The SLD Collaboration*

Abstract

The lifetimes of B^+ and B^0 mesons have been measured using a sample of 150,000 hadronic Z^0 decays collected by the SLD experiment at the SLC between 1993 and 1995. The analysis identifies the semileptonic decays of B mesons with high (p, p_t) leptons and reconstructs the B meson decay length and charge by vertexing the lepton with a partially reconstructed D meson. This method results in a sample of 634 (584) charged (neutral) decays with high charge purity. A maximum likelihood fit finds: $\tau_{B^+} = 1.60^{+0.12}_{-0.11}(\text{stat}) \pm 0.06(\text{syst})$ ps, $\tau_{B^0} = 1.55^{+0.13}_{-0.12}(\text{stat}) \pm 0.09(\text{syst})$ ps, and the ratio $\tau_{B^+}/\tau_{B^0} = 1.03^{+0.15}_{-0.13}(\text{stat}) \pm 0.08(\text{syst})$.

*Paper Contributed to the XXVIII International Conference on High Energy
Physics, July 25-31, 1996, Warsaw, Poland*

**This work was supported by Department of Energy contracts: DE-FG02-91ER40676 (BU), DE-FG03-92ER40701 (CIT), DE-FG03-91ER40618 (UCSB), DE-FG03-92ER40689 (UCSC), DE-FG03-93ER40788 (CSU), DE-FG02-91ER40672 (Colorado), DE-FG02-91ER40677 (Illinois), DE-AC03-76SF00098 (LBL), DE-FG02-92ER40715 (Massachusetts), DE-AC02-76ER03069 (MIT), DE-FG06-85ER40224 (Oregon), DE-AC03-76SF00515 (SLAC), DE-FG05-91ER40627 (Tennessee), DE-AC02-76ER00881 (Wisconsin), DE-FG02-92ER40704 (Yale); National Science Foundation grants: PHY-91-13428 (UCSC), PHY-89-21320 (Columbia), PHY-92-04239 (Cincinnati), PHY-88-17930 (Rutgers), PHY-88-19316 (Vanderbilt), PHY-92-03212 (Washington); the UK Science and Engineering Research Council (Brunel and RAL); the Istituto Nazionale di Fisica Nucleare of Italy (Bologna, Ferrara, Frascati, Pisa, Padova, Perugia); and the Japan-US Cooperative Research Project on High Energy Physics (Nagoya, Tohoku).

According to the spectator model of heavy hadron decay, the heavy quark is considered to decay weakly independently of the other light quarks in the hadron. This model predicts that the lifetimes of all hadrons containing a given heavy quark Q are determined by the lifetime of that quark and are, therefore, equal. However, the hierarchy observed in the charm system, $\tau_{D^+} > \tau_{D_s^+} \sim \tau_{D^0} > \tau_{\Lambda_c^+}$, indicates the need for corrections to this model. In the b -quark system a similar hierarchy, $\tau_{B^+} > \tau_{B_s^0} \sim \tau_{B^0} > \tau_{\Lambda_b^0}$, is expected. Here the lifetime differences are expected to be less than 10% since they scale with $1/m_Q^2$. A QCD calculation [1] using an expansion in the inverse powers of the b -quark mass predicts $\tau_{B^+}/\tau_{B^0} = 1.0 + 0.05 \times \left(\frac{f_B}{200 \text{ MeV}}\right)^2$, where f_B is the B meson decay constant. Thus, measurements of the B^+ and B^0 lifetimes and their ratio provide tests of deviations from the spectator model.

The B^+ and B^0 lifetime measurements presented here use a sample of 150,000 hadronic Z^0 decays collected between 1993 and 1995 by the SLD experiment at the SLAC Linear Collider (SLC). The goal of this analysis is to reconstruct the charged track topology of semileptonic B decays. The algorithm reconstructs both B and cascade D vertices. The B vertex contains the lepton and at most one other track, and the D vertex contains two, three or four tracks. This new topological technique does not use the charge correlation between the lepton and the D vertex but simply determines the total charge of the B meson from the sum of charges in the B and D vertices. The final charge assignment purity will be somewhat diluted, however, due to the fraction of decays of the type $B^+ \rightarrow \bar{D}^{*0} l^+ \nu$ which can yield two slow transition pions at the B vertex. (Charge conjugation is implied throughout this paper.)

This analysis relies on SLD's calorimetry and tracking systems (detailed descriptions can be found in Ref. [2]). The Liquid Argon Calorimeter (LAC) provides excellent solid-angle coverage ($|\cos \theta| < 0.84$ and $0.82 < |\cos \theta| < 0.98$ in the barrel and endcap regions, respectively). The Warm Iron Calorimeter (WIC) also covers much of the solid-angle ($|\cos \theta| < 0.95$) and provides maximal muon identification efficiency for $|\cos \theta| < 0.60$. The LAC is divided longitudinally into electromagnetic and hadronic sections. The energy resolution for electromagnetic showers is measured to be $\sigma/E = 15\%/\sqrt{E(\text{GeV})}$, whereas that for hadronic showers is estimated to be $60\%/\sqrt{E(\text{GeV})}$. Tracking is provided by the Central Drift Chamber (CDC) and the CCD pixel Vertex Detector (VXD) with maximal track reconstruction efficiency for $|\cos \theta| < 0.74$. Charged tracks are first reconstructed in the CDC and linked with clusters in the VXD, and then a combined fit is performed. The momentum resolution of the combined fit is $\sigma_{p_T}/p_T = \sqrt{(0.01)^2 + (0.0026/p_T)^2}$, where p_T is the track momentum transverse to the beam direction in GeV/c . The impact parameter resolution was measured using the miss distance between the two tracks in $Z^0 \rightarrow \mu^+ \mu^-$ decays. This yields a high-momentum single-track resolution of 11 μm in the plane perpendicular to the beam direction (xy plane) and 38 μm in the plane containing the beam axis (rz plane).

The position of the micron-sized SLC Interaction Point (IP) in the xy plane is reconstructed with a measured precision of $\sigma_{IP} = (7 \pm 2) \mu\text{m}$ using tracks in sets of ~ 30 sequential hadronic Z^0 decays. The z position of the Z^0 primary vertex is determined on an event-by-event basis using the median z position of tracks at their point-of-closest-approach to the IP in the xy plane. The simulation described below estimates a precision of $\sim 52 \mu\text{m}$ in this quantity for $Z^0 \rightarrow b \bar{b}$ decays [2].

The lifetime measurements rely on a Monte Carlo simulation based on the JETSET 7.4 event generator [3] and the GEANT 3.21 detector simulation package [4]. The b -quark fragmentation followed the Peterson *et al.* parametrization [5]. B mesons were generated with mean lifetime $\tau = 1.55$ ps and B baryons with $\tau = 1.10$ ps. B hadron decays were modelled according to the CLEO B decay model [6] tuned to reproduce the spectra and multiplicities of leptons, charmed hadrons, pions, kaons, and protons, measured at the $\Upsilon(4S)$ by ARGUS and CLEO [7, 8]. B baryon and charmed hadron decays were modelled using JETSET with, in the latter case, branching fractions tuned to existing measurements [9].

A discrepancy between data and simulation was observed in the fraction of tracks passing a set of quality cuts. This effect was corrected for by removing the appropriate number of tracks from the simulation, taking into account the dependence of the effect on track p_T , $\cos \theta$, azimuthal angle and angle between the track and the nearest jet axis. The overall effect was to remove 3.8% of the Monte Carlo tracks used in this analysis. Furthermore, there remained a discrepancy between data and simulation in the distribution of number of tracks attached to reconstructed vertices (see below for a description of the vertex reconstruction algorithm). Although this effect could be partly due to the modeling of B and D decays, we conservatively assumed the discrepancy to be entirely due to a lower vertex reconstruction efficiency in the data. To correct for this, an efficiency of 90% (81%) was applied to reconstructed 3-prong (4-prong) vertices in the simulation. The effect of these track and vertex efficiency corrections is investigated as part of the systematic error study below.

The initial step in this analysis is to identify a lepton candidate originating from the decay of a B meson. Electron candidates are required to have a measured energy in the LAC which agrees with the momentum of the associated track measured in the CDC, to have little or no LAC hadronic energy, and to have a front/back electromagnetic energy ratio consistent with that expected for electrons [10]. Muon candidates are required to have a good match between hits found in the WIC and tracks extrapolated from the CDC, taking into account track extrapolation errors and multiple scattering [10]. To enhance the fraction of $Z^0 \rightarrow b \bar{b}$ events with relatively small loss in efficiency, lepton candidates are required to pass relatively loose cuts: total momentum $p > 2 \text{ GeV}/c$ and momentum transverse to the nearest jet $> 0.4 \text{ GeV}/c$ (where jets are found from calorimeter clusters using the JADE algorithm [11] with $y_{cut} = 0.005$). Application of these cuts yields a sample of 34K events, including approximately 75% of the electrons and muons from semileptonic

B decays within $|\cos\theta| < 0.6$.

The B and D decay vertex reconstruction proceeds separately for each event hemisphere containing a lepton using a multi-pass algorithm which operates on those tracks which have at least one VXD hit and are classified as either primary or secondary. The first step of this track classification scheme is to remove tracks from identified γ conversions, or from identified K^0 or Λ decays. The remaining tracks are classified as primary unless their 3-D impact parameter with respect to the primary vertex $> 3.5\sigma$ and their momentum $p > 0.8$ GeV/ c , in which case they are classified as secondary.

In the first pass, the event hemisphere containing the lepton candidate is required to contain no more than four secondary tracks (excluding the lepton) and a D vertex is constructed using all such tracks (vertex cuts are defined below). The D trajectory, found from the D vertex and the total momentum vector of tracks included in the vertex, must intersect the lepton to form a valid (one-prong) B vertex solution. If this step is successful, an attempt is made to form a two-prong B vertex by attaching one primary track to the lepton near the point of intersection. This first pass identifies 91% of the final candidates. In the second pass, the first pass successes are allowed to be modified by searching for primary tracks which can be added to the existing D vertex. This search is successful for 40% of the initial pass 1 candidates and they are reclassified as pass 2. Multiple solutions are sorted on the basis of the smallest impact parameter between the D trajectory and the lepton or B vertex. The third pass is performed on those hemispheres in which no pass 1 candidate was identified. In this pass, a search is made for solutions in which one secondary track makes a valid B vertex with the lepton, the remaining secondary tracks form a D vertex, and the D trajectory intersects the B vertex. This third pass identifies the remaining 9% of the final candidates. In all passes, at most one track is added to the lepton to form the B vertex and at most two tracks are added to the original D vertex.

The requirements for tracks to form a D vertex are: the absolute value of the charge ≤ 1 , the mass (charged tracks assumed to be π 's) < 1.98 GeV, the vertex displacement from the IP $> 4\sigma$ and < 2.5 cm, and the vertex χ^2 (2,3,4 prongs) $< (4, 12, 20)$. The requirements for tracks to form a B vertex are: the absolute value of the total charge ($B + D$) ≤ 1 , the mass ($B + D$ tracks) > 1.4 GeV, the observed decay length (displacement from IP) > 0.08 cm and < 2.4 cm, and the momentum of the non-lepton track (if any) > 0.4 GeV/ c . The requirements for the D vertex to be linked to the B vertex are: the distance between D and B vertices > 200 μm , and for one-prong B , the distance of closest approach of the D vector with the lepton, $< (130, 100, 70)$ μm for (2, 3, 4) prong D vertices, while for two-prong B , the three-dimensional impact parameter of the D vector with respect to the B vertex < 200 μm .

The analysis described above isolates 1367 semileptonic B decay candidates. Of these, 783 are reconstructed as charged decays and 584 as neutral decays, with the

topological breakdown given in Table 1 together with predictions from the simulation. Using the Monte Carlo simulation, the efficiency for reconstructing a semileptonic B decay is estimated to be 24% for decays with an identified lepton within $|\cos \theta| < 0.6$.

Monte Carlo studies indicate that the B^+ topology consisting of two-prong B and three-prong D vertices has very poor B^+ purity due to the relatively small (expected) branching ratio for $B^+ \rightarrow D^+ \pi^- l^+ \nu$. Therefore, this topology is rejected for the remainder of the analysis. The number of decays reconstructed as charged is thus reduced from 783 to 634. Monte Carlo studies show that the remaining charged (neutral) sample is 97.5% (99.1%) pure in B hadrons. The simulated flavor contents are 66.9% B_u^+ , 22.5% B_d^0 , 5.7% B_s^0 , and 2.4% B baryons for the charged sample, and 19.6% B_u^+ , 60.8% B_d^0 , 14.0% B_s^0 , and 4.7% B baryons for the neutral sample. The sensitivity of this analysis to the individual B_u^+ and B_d^0 lifetimes can be assessed from the 3:1 ratio of B_u^+ (B_d^0) decays over B_d^0 (B_u^+) decays in the charged (neutral) sample. The rate of lepton misidentification is 7.1% (10.2%) for charged (neutral) decays, as determined from our simulation. However, these are still mostly B decays with good charge purity.

As a check of the charge assignment algorithm, the requirement on the charge of the B and D vertices is removed and the Monte Carlo simulation is compared with the data. The charge reconstruction performance can be evaluated by comparing the charges of the lepton and D vertex. These are expected to be opposite (provided the D vertex is charged) as evidenced by Fig. 1(a) which shows the product of the lepton and D vertex charges. Furthermore, the charge distribution resulting from the lepton+slow transition pion vertex (from D^* and D^{**}) is shown in Fig. 1(b) and displays excellent agreement between data and simulation. Fig. 1(b) indicates that the track combined with the lepton to form a two-prong B vertex most often has charge opposite that of the lepton, as expected for $B \rightarrow D^* l \nu$ decays and most $B \rightarrow D^{**} l \nu$ decays. Figure 1 also shows the D vertex multiplicity distribution, and the invariant mass and total momentum distributions obtained using the tracks from both B and D vertices (with the nominal charge requirement on the vertices). Overall, there is good agreement between the data and the Monte Carlo simulation.

Another check of the charge assignment algorithm is performed by forming the Forward-Backward asymmetry using the thrust axis to approximate the angle (θ_T) the b quark makes with the electron beam and using the charge of the lepton to determine the charge of the b quark. This asymmetry is formed separately for the left and right handed electron polarizations and for decays reconstructing as charged and neutral. The left and right samples are combined to form the Left-Right Forward-Backward asymmetries [10] for charged and neutral decays, as shown in figure 2. The presence of $B^0 - \bar{B}^0$ mixing causes the dilution of the asymmetry observable in the neutral plot. In the limit of random charge assignment both plots would display the same asymmetry. Figure 2 also shows the good agreement between the data and the simulation for the asymmetries.

The B^+ and B^0 lifetimes are extracted from the decay length distribution of the reconstructed B vertices using a binned maximum likelihood technique. The distributions for the charged and neutral samples, shown in Fig. 3, are fitted simultaneously to determine two parameters: the lifetime ratio τ_{B^+}/τ_{B^0} and either the B^+ or the B^0 lifetime (the results do not depend on which set of two parameters are used in the fit). The values of the ratio are varied between 0.6 and 1.4, and the B^+ or B^0 lifetimes are varied between 1.0 and 2.0 ps in the fit. For each set of parameters, Monte Carlo decay length distributions are obtained by reweighting the original Monte Carlo decay length distributions for B^+ and B^0 with

$$W(t, \tau) = \frac{\frac{1}{\tau} e^{-t/\tau}}{\frac{1}{\tau_{gen}} e^{-t/\tau_{gen}}}, \quad (1)$$

where τ is the desired B^+ or B^0 lifetime, τ_{gen} is the lifetime value used in the Monte Carlo generation, i.e. 1.55 ps, and t is the proper time of each decay.

The maximum likelihood fit yields $\tau_{B^+} = 1.60^{+0.12}_{-0.11}$ ps and $\tau_{B^0} = 1.55^{+0.13}_{-0.12}$ ps, with a lifetime ratio $\frac{\tau_{B^+}}{\tau_{B^0}} = 1.03^{+0.15}_{-0.13}$. The best fit Monte Carlo distributions (the overlays in Fig. 3) give a $\chi^2 = 80$ for 76 degrees of freedom for the combined fit to both charged and neutral distributions. As a check, the fit was performed for decays in four different azimuthal ranges. All fit results were found to be consistent with the nominal results within statistical uncertainties.

Systematic uncertainties due to detector and physics modeling, as well as those related to the fitting procedure, have been investigated. The individual contributions to the total systematic uncertainty in the B^+ and B^0 lifetimes and their ratio are summarized in Table 2.

The main contribution to the systematic error due to detector modeling originates from the uncertainty in the track and vertex reconstruction efficiency. This was taken to be the difference between fit results obtained with and without the track and vertexing efficiency corrections in the simulation. Distributions of the track impact parameters in the rz plane indicate a narrower core in the simulation than in the data. The degraded resolution in the data is attributed to residual misalignments within the VXD ladders. The resolution uncertainty was estimated by correcting the z coordinates of tracks in the Monte Carlo simulation [2]. The uncertainty in the rate of fake lepton identification was investigated by varying this rate by $\pm 25\%$ in the simulation.

The contributions to the systematic error due to physics modeling include the uncertainties in the b -quark fragmentation and the B meson decay model, as well as the sensitivity to assumptions concerning B_s and B baryon production and lifetimes. The uncertainty in b -quark fragmentation was determined by varying the ϵ_b parameter in the Peterson fragmentation function [5], corresponding to $\langle x_E \rangle = 0.700 \pm 0.011$ [12]. The systematic error also includes a variation in the shape of the x_E distribution [13]. The branching ratio for decays involving $b \rightarrow c \rightarrow l$ transitions was

varied by $\pm 10\%$ relative. This variation was applied in an anticorrelated way for B^+ and B^0 decays. Variation of the branching ratio for $B \rightarrow \tau \nu_\tau X$ according to the uncertainty in the current world average [9] was found to have a negligible effect. The branching ratio for $B \rightarrow DDX$ was varied according to 0.15 ± 0.05 . The sensitivity to $B \rightarrow \tau \nu_\tau X$ was found to be negligible. We also investigated the sensitivity to $B \rightarrow D^{**} l \nu$ decays which produce two slow charged pions at the B decay vertex in about 8% of all semileptonic decays in our simulation. The branching ratio for $B \rightarrow D^{**} l \nu$ decays was varied by $\pm 50\%$ relative. The sensitivity to the charm decay modeling was studied by varying the number of tracks produced in decays of charm hadrons according to the uncertainty in the corresponding measurement [14]. The lifetime fit assumes particular values for the B_s and B baryon lifetimes and production fractions. These were varied according to $\tau(B_s) = 1.55 \pm 0.15$ ps, $\tau(B \text{ baryon}) = 1.10 \pm 0.11$ ps, $f(B_s) = 0.12 \pm 0.04$, and $f(B \text{ baryon}) = 0.08 \pm 0.04$. Finally, the lifetime of charm hadrons (D^+ , D^0 , D_s , Λ_c) was varied according to the uncertainty in their world average values [9].

The largest contributions to the systematic error arise from uncertainties in the fitting procedure and from Monte Carlo statistics. The fitting uncertainties were estimated by varying the bin size used in the decay length fit distributions, and by modifying the cuts on the minimum and maximum decay lengths used in the fit. Although the lifetimes obtained for each of these variations were statistically consistent with the nominal lifetime, we have conservatively assigned a systematic uncertainty equal to the root mean square value of all these fit results.

The results of these systematic studies are used to obtain the following preliminary results:

$$\begin{aligned}\tau_{B^+} &= 1.60_{-0.11}^{+0.12}(\text{stat}) \pm 0.06(\text{syst}) \text{ ps}, \\ \tau_{B^0} &= 1.55_{-0.12}^{+0.13}(\text{stat}) \pm 0.09(\text{syst}) \text{ ps},\end{aligned}$$

with a ratio of:

$$\frac{\tau_{B^+}}{\tau_{B^0}} = 1.03_{-0.13}^{+0.15}(\text{stat}) \pm 0.08(\text{syst}).$$

These results are in good agreement with the current world averages and with the expectation that B^+ and B^0 lifetimes are nearly equal.

We thank the personnel of the SLAC accelerator department and the technical staffs of our collaborating institutions for their outstanding efforts.

References

- [1] *Non-leptonic Decays of Beauty Hadrons - from Phenomenology to Theory*, I.I. Bigi *et al.*, in *B Decays*, ed. S. Stone, World Scientific (1994); *Lifetimes of Heavy Flavor Hadrons: Whence and Whither?* I.I. Bigi, UND-HEP-95-BIG-06 (1995).

- [2] K. Abe *et al.*, Phys. Rev. **D53**, 1023 (1996).
- [3] T. Sjöstrand, CERN-TH-7112-93, Feb. 1994.
- [4] R. Brun *et al.*, CERN-DD/EE/84-1, 1989.
- [5] C. Peterson *et al.*, Phys. Rev. **D27**, 105 (1983).
- [6] CLEO QQ MC code provided by P. Kim and the CLEO Collaboration.
- [7] CLEO Collaboration: B. Barish *et al.*, **CLNS-95-1362** (1995);
 ARGUS Collaboration: H. Albrecht *et al.*, *Z. Phys.* **C58**, 191 (1993);
 ARGUS Collaboration: H. Albrecht *et al.*, *Z. Phys.* **C62**, 371 (1994);
 F. Muheim (CLEO Collaboration), talk presented at the 8th DPF Meeting,
 Albuquerque, New Mexico, Aug 1994;
 M. Thulasidas, Ph.D thesis, Syracuse University (1993);
 CLEO Collaboration: G. Crawford *et al.*, *Phys. Rev.* **D45**, 752 (1992)
 CLEO Collaboration: D. Bortoletto *et al.*, *Phys. Rev.* **D45**, 21 (1992).
- [8] T.R. Junk, Ph.D. Thesis, Stanford University, SLAC-Report-95-476, Nov. 1995.
- [9] Particle Data Group, Phys. Rev. **D50**, Part I (1994).
- [10] K. Abe *et al.*, Phys. Rev. Lett. **74**, 2895 (1995).
- [11] S. Bethke *et al.*, Phys. Lett. **213B**, 235 (1988).
- [12] see for example,
 R. Akers *et al.*, *Z. Phys.* **C60**, 199 (1993);
 D. Buskulic *et al.*, *Z. Phys.* **C62**, 179 (1994);
 P. Abreu *et al.*, *Z. Phys.* **C66**, 323 (1995).
- [13] M. G. Bowler, *Z. Phys.* **C11**, 169 (1981).
- [14] D.Coffman *et al.*, Phys. Lett. **B263**, 135 (1991);

*List of Authors

K. Abe,⁽¹⁹⁾ K. Abe,⁽²⁹⁾ I. Abt,⁽¹³⁾ T. Akagi,⁽²⁷⁾ N.J. Allen,⁽⁴⁾ W.W. Ash,^{(27)†}
 D. Aston,⁽²⁷⁾ K.G. Baird,⁽²⁴⁾ C. Baltay,⁽³³⁾ H.R. Band,⁽³²⁾ M.B. Barakat,⁽³³⁾
 G. Baranko,⁽⁹⁾ O. Bardon,⁽¹⁵⁾ T. Barklow,⁽²⁷⁾ A.O. Bazarko,⁽¹⁰⁾ R. Ben-David,⁽³³⁾
 A.C. Benvenuti,⁽²⁾ G.M. Bilei,⁽²²⁾ D. Bisello,⁽²¹⁾ G. Blaylock,⁽⁶⁾ J.R. Bogart,⁽²⁷⁾
 B. Bolen,⁽¹⁷⁾ T. Bolton,⁽¹⁰⁾ G.R. Bower,⁽²⁷⁾ J.E. Brau,⁽²⁰⁾ M. Breidenbach,⁽²⁷⁾
 W.M. Bugg,⁽²⁸⁾ D. Burke,⁽²⁷⁾ T.H. Burnett,⁽³¹⁾ P.N. Burrows,⁽¹⁵⁾ W. Busza,⁽¹⁵⁾
 A. Calcaterra,⁽¹²⁾ D.O. Caldwell,⁽⁵⁾ D. Calloway,⁽²⁷⁾ B. Camanzi,⁽¹¹⁾
 M. Carpinelli,⁽²³⁾ R. Cassell,⁽²⁷⁾ R. Castaldi,^{(23)(a)} A. Castro,⁽²¹⁾
 M. Cavalli-Sforza,⁽⁶⁾ A. Chou,⁽²⁷⁾ E. Church,⁽³¹⁾ H.O. Cohn,⁽²⁸⁾ J.A. Coller,⁽³⁾

V. Cook,⁽³¹⁾ R. Cotton,⁽⁴⁾ R.F. Cowan,⁽¹⁵⁾ D.G. Coyne,⁽⁶⁾ G. Crawford,⁽²⁷⁾
 A. D'Oliveira,⁽⁷⁾ C.J.S. Damerell,⁽²⁵⁾ M. Daoudi,⁽²⁷⁾ R. De Sangro,⁽¹²⁾
 R. Dell'Orso,⁽²³⁾ P.J. Dervan,⁽⁴⁾ M. Dima,⁽⁸⁾ D.N. Dong,⁽¹⁵⁾ P.Y.C. Du,⁽²⁸⁾
 R. Dubois,⁽²⁷⁾ B.I. Eisenstein,⁽¹³⁾ R. Elia,⁽²⁷⁾ E. Etzion,⁽⁴⁾ D. Falciari,⁽²²⁾ C. Fan,⁽⁹⁾
 M.J. Fero,⁽¹⁵⁾ R. Frey,⁽²⁰⁾ K. Furuno,⁽²⁰⁾ T. Gillman,⁽²⁵⁾ G. Gladding,⁽¹³⁾
 S. Gonzalez,⁽¹⁵⁾ G.D. Hallewell,⁽²⁷⁾ E.L. Hart,⁽²⁸⁾ J.L. Harton,⁽⁸⁾ A. Hasan,⁽⁴⁾
 Y. Hasegawa,⁽²⁹⁾ K. Hasuko,⁽²⁹⁾ S. J. Hedges,⁽³⁾ S.S. Hertzbach,⁽¹⁶⁾
 M.D. Hildreth,⁽²⁷⁾ J. Huber,⁽²⁰⁾ M.E. Huffer,⁽²⁷⁾ E.W. Hughes,⁽²⁷⁾ H. Hwang,⁽²⁰⁾
 Y. Iwasaki,⁽²⁹⁾ D.J. Jackson,⁽²⁵⁾ P. Jacques,⁽²⁴⁾ J. A. Jaros,⁽²⁷⁾ A.S. Johnson,⁽³⁾
 J.R. Johnson,⁽³²⁾ R.A. Johnson,⁽⁷⁾ T. Junk,⁽²⁷⁾ R. Kajikawa,⁽¹⁹⁾ M. Kallelkar,⁽²⁴⁾
 H. J. Kang,⁽²⁶⁾ I. Karliner,⁽¹³⁾ H. Kawahara,⁽²⁷⁾ H.W. Kendall,⁽¹⁵⁾ Y. D. Kim,⁽²⁶⁾
 M.E. King,⁽²⁷⁾ R. King,⁽²⁷⁾ R.R. Kofler,⁽¹⁶⁾ N.M. Krishna,⁽⁹⁾ R.S. Kroeger,⁽¹⁷⁾
 J.F. Labs,⁽²⁷⁾ M. Langston,⁽²⁰⁾ A. Lath,⁽¹⁵⁾ J.A. Lauber,⁽⁹⁾ D.W.G.S. Leith,⁽²⁷⁾
 V. Lia,⁽¹⁵⁾ M.X. Liu,⁽³³⁾ X. Liu,⁽⁶⁾ M. Loreti,⁽²¹⁾ A. Lu,⁽⁵⁾ H.L. Lynch,⁽²⁷⁾ J. Ma,⁽³¹⁾
 G. Mancinelli,⁽²²⁾ S. Manly,⁽³³⁾ G. Mantovani,⁽²²⁾ T.W. Markiewicz,⁽²⁷⁾
 T. Maruyama,⁽²⁷⁾ H. Masuda,⁽²⁷⁾ E. Mazzucato,⁽¹¹⁾ A.K. McKemey,⁽⁴⁾
 B.T. Meadows,⁽⁷⁾ R. Messner,⁽²⁷⁾ P.M. Mockett,⁽³¹⁾ K.C. Moffeit,⁽²⁷⁾
 T.B. Moore,⁽³³⁾ D. Muller,⁽²⁷⁾ T. Nagamine,⁽²⁷⁾ S. Narita,⁽²⁹⁾ U. Nauenberg,⁽⁹⁾
 H. Neal,⁽²⁷⁾ M. Nussbaum,⁽⁷⁾ Y. Ohnishi,⁽¹⁹⁾ L.S. Osborne,⁽¹⁵⁾ R.S. Panvini,⁽³⁰⁾
 H. Park,⁽²⁰⁾ T.J. Pavel,⁽²⁷⁾ I. Peruzzi,^{(12)(b)} M. Piccolo,⁽¹²⁾ L. Piemontese,⁽¹¹⁾
 E. Pieroni,⁽²³⁾ K.T. Pitts,⁽²⁰⁾ R.J. Plano,⁽²⁴⁾ R. Prepost,⁽³²⁾ C.Y. Prescott,⁽²⁷⁾
 G.D. Punkar,⁽²⁷⁾ J. Quigley,⁽¹⁵⁾ B.N. Ratcliff,⁽²⁷⁾ T.W. Reeves,⁽³⁰⁾ J. Reidy,⁽¹⁷⁾
 P.E. Rensing,⁽²⁷⁾ L.S. Rochester,⁽²⁷⁾ P.C. Rowson,⁽¹⁰⁾ J.J. Russell,⁽²⁷⁾
 O.H. Saxton,⁽²⁷⁾ T. Schalk,⁽⁶⁾ R.H. Schindler,⁽²⁷⁾ B.A. Schumm,⁽¹⁴⁾ S. Sen,⁽³³⁾
 V.V. Serbo,⁽³²⁾ M.H. Shaevitz,⁽¹⁰⁾ J.T. Shank,⁽³⁾ G. Shapiro,⁽¹⁴⁾ D.J. Sherden,⁽²⁷⁾
 K.D. Shmakov,⁽²⁸⁾ C. Simopoulos,⁽²⁷⁾ N.B. Sinev,⁽²⁰⁾ S.R. Smith,⁽²⁷⁾ M.B. Smy,⁽⁸⁾
 J.A. Snyder,⁽³³⁾ P. Stamer,⁽²⁴⁾ H. Steiner,⁽¹⁴⁾ R. Steiner,⁽¹⁾ M.G. Strauss,⁽¹⁶⁾
 D. Su,⁽²⁷⁾ F. Suekane,⁽²⁹⁾ A. Sugiyama,⁽¹⁹⁾ S. Suzuki,⁽¹⁹⁾ M. Swartz,⁽²⁷⁾
 A. Szumilo,⁽³¹⁾ T. Takahashi,⁽²⁷⁾ F.E. Taylor,⁽¹⁵⁾ E. Torrence,⁽¹⁵⁾ A.I. Trandafir,⁽¹⁶⁾
 J.D. Turk,⁽³³⁾ T. Usher,⁽²⁷⁾ J. Va'vra,⁽²⁷⁾ C. Vannini,⁽²³⁾ E. Vella,⁽²⁷⁾
 J.P. Venuti,⁽³⁰⁾ R. Verdier,⁽¹⁵⁾ P.G. Verdini,⁽²³⁾ S.R. Wagner,⁽²⁷⁾ A.P. Waite,⁽²⁷⁾
 S.J. Watts,⁽⁴⁾ A.W. Weidemann,⁽²⁸⁾ E.R. Weiss,⁽³¹⁾ J.S. Whitaker,⁽³⁾
 S.L. White,⁽²⁸⁾ F.J. Wickens,⁽²⁵⁾ D.A. Williams,⁽⁶⁾ D.C. Williams,⁽¹⁵⁾
 S.H. Williams,⁽²⁷⁾ S. Willocq,⁽³³⁾ R.J. Wilson,⁽⁸⁾ W.J. Wisniewski,⁽²⁷⁾
 M. Woods,⁽²⁷⁾ G.B. Word,⁽²⁴⁾ J. Wyss,⁽²¹⁾ R.K. Yamamoto,⁽¹⁵⁾ J.M. Yamartino,⁽¹⁵⁾
 X. Yang,⁽²⁰⁾ S.J. Yellin,⁽⁵⁾ C.C. Young,⁽²⁷⁾ H. Yuta,⁽²⁹⁾ G. Zapalac,⁽³²⁾
 R.W. Zdarko,⁽²⁷⁾ C. Zeitlin,⁽²⁰⁾ and J. Zhou,⁽²⁰⁾

⁽¹⁾ *Adelphi University, Garden City, New York 11530*

⁽²⁾ *INFN Sezione di Bologna, I-40126 Bologna, Italy*

⁽³⁾ *Boston University, Boston, Massachusetts 02215*

⁽⁴⁾ *Brunel University, Uxbridge, Middlesex UB8 3PH, United Kingdom*

⁽⁵⁾ *University of California at Santa Barbara, Santa Barbara, California 93106*

- (⁶) *University of California at Santa Cruz, Santa Cruz, California 95064*
 (⁷) *University of Cincinnati, Cincinnati, Ohio 45221*
 (⁸) *Colorado State University, Fort Collins, Colorado 80523*
 (⁹) *University of Colorado, Boulder, Colorado 80309*
 (¹⁰) *Columbia University, New York, New York 10027*
 (¹¹) *INFN Sezione di Ferrara and Università di Ferrara, I-44100 Ferrara, Italy*
 (¹²) *INFN Lab. Nazionali di Frascati, I-00044 Frascati, Italy*
 (¹³) *University of Illinois, Urbana, Illinois 61801*
 (¹⁴) *Lawrence Berkeley Laboratory, University of California, Berkeley, California 94720*
 (¹⁵) *Massachusetts Institute of Technology, Cambridge, Massachusetts 02139*
 (¹⁶) *University of Massachusetts, Amherst, Massachusetts 01003*
 (¹⁷) *University of Mississippi, University, Mississippi 38677*
 (¹⁹) *Nagoya University, Chikusa-ku, Nagoya 464 Japan*
 (²⁰) *University of Oregon, Eugene, Oregon 97403*
 (²¹) *INFN Sezione di Padova and Università di Padova, I-35100 Padova, Italy*
 (²²) *INFN Sezione di Perugia and Università di Perugia, I-06100 Perugia, Italy*
 (²³) *INFN Sezione di Pisa and Università di Pisa, I-56100 Pisa, Italy*
 (²⁴) *Rutgers University, Piscataway, New Jersey 08855*
 (²⁵) *Rutherford Appleton Laboratory, Chilton, Didcot, Oxon OX11 0QX United Kingdom*
 (²⁶) *Sogang University, Seoul, Korea*
 (²⁷) *Stanford Linear Accelerator Center, Stanford University, Stanford, California 94309*
 (²⁸) *University of Tennessee, Knoxville, Tennessee 37996*
 (²⁹) *Tohoku University, Sendai 980 Japan*
 (³⁰) *Vanderbilt University, Nashville, Tennessee 37235*
 (³¹) *University of Washington, Seattle, Washington 98195*
 (³²) *University of Wisconsin, Madison, Wisconsin 53706*
 (³³) *Yale University, New Haven, Connecticut 06511*
 † *Deceased*
 (^a) *Also at the Università di Genova*
 (^b) *Also at the Università di Perugia*

	<i>B</i> Vertex	<i>D</i> Vertex		Data	MC
<i>B</i> ⁺	1 prong	2 prong	519	(38.0 ± 1.3)%	38.2%
	1 prong	4 prong	115	(8.4 ± 0.8)%	8.4%
	2 prong	3 prong	149	(10.9 ± 0.8)%	9.3%
<i>B</i> ⁰	1 prong	3 prong	341	(24.9 ± 1.2)%	27.1%
	2 prong	2 prong	175	(12.8 ± 0.9)%	13.3%
	2 prong	4 prong	68	(5.0 ± 0.6)%	3.7%

Table 1: Summary of reconstructed topologies, including the fraction of each topology in the combined charged and neutral semileptonic *B* decay sample for data and Monte Carlo simulation.

Systematic Error	$\Delta\tau_{B^+}$ (ps)	$\Delta\tau_{B^0}$ (ps)	$\Delta\left(\frac{\tau^+}{\tau^0}\right)$
Detector Modeling			
Track efficiency	0.006	0.029	0.023
Detector resolution	0.004	0.027	0.020
Lepton ID	0.006	0.006	0.001
Physics Modeling			
<i>b</i> fragmentation	0.034	0.036	0.004
BR(<i>B</i> → <i>D</i> ** <i>lνX</i>)	0.010	0.008	0.011
BR(<i>B</i> → <i>DDX</i>)	0.009	0.008	0.011
BR(<i>B</i> → <i>X</i> → <i>l</i>)	0.001	0.001	0.001
<i>B_s</i> fraction	0.009	0.005	0.009
<i>B</i> baryon fraction	0.009	0.015	0.004
<i>B_s</i> lifetime	0.002	0.035	0.024
<i>B</i> baryon lifetime	0.001	0.011	0.008
<i>D</i> multiplicity	0.013	0.011	0.001
Charm hadron lifetime	0.004	0.003	0.003
Monte Carlo and Fitting			
Fit systematics	0.038	0.042	0.056
MC statistics	0.030	0.033	0.038
TOTAL	0.064	0.087	0.081

Table 2: Summary of contributions to the systematic uncertainty in the *B*⁺ and *B*⁰ lifetimes and their ratio.

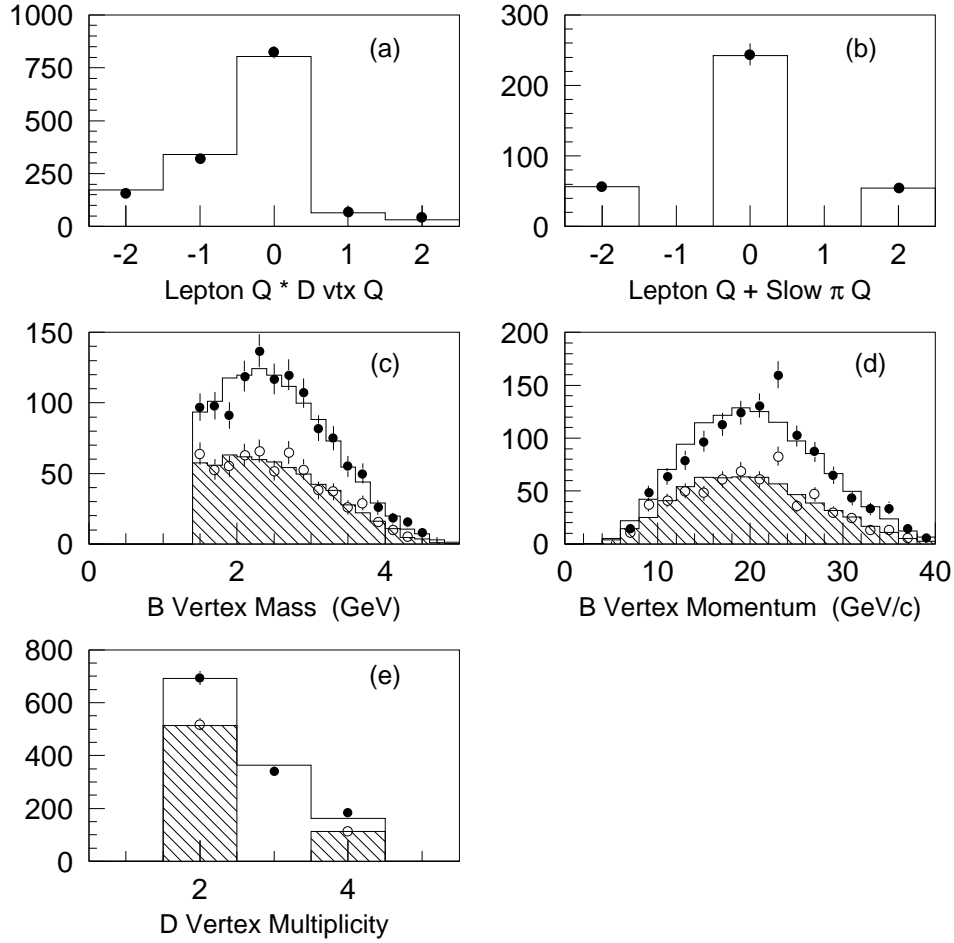


Figure 1: Distributions of the product between lepton and D vertex charges (a) and sum of lepton and slow transition pion charges (b) for data (points) and Monte Carlo simulation (histograms) with no charge requirement at the B and D vertices, and distributions of B vertex mass (c), B vertex momentum (d) and D vertex multiplicity (e) for data (solid circles are for charged and neutral samples, open circles are for charged sample only) and Monte Carlo simulation (histograms are for charged and neutral samples, shaded portions are for charged sample only).

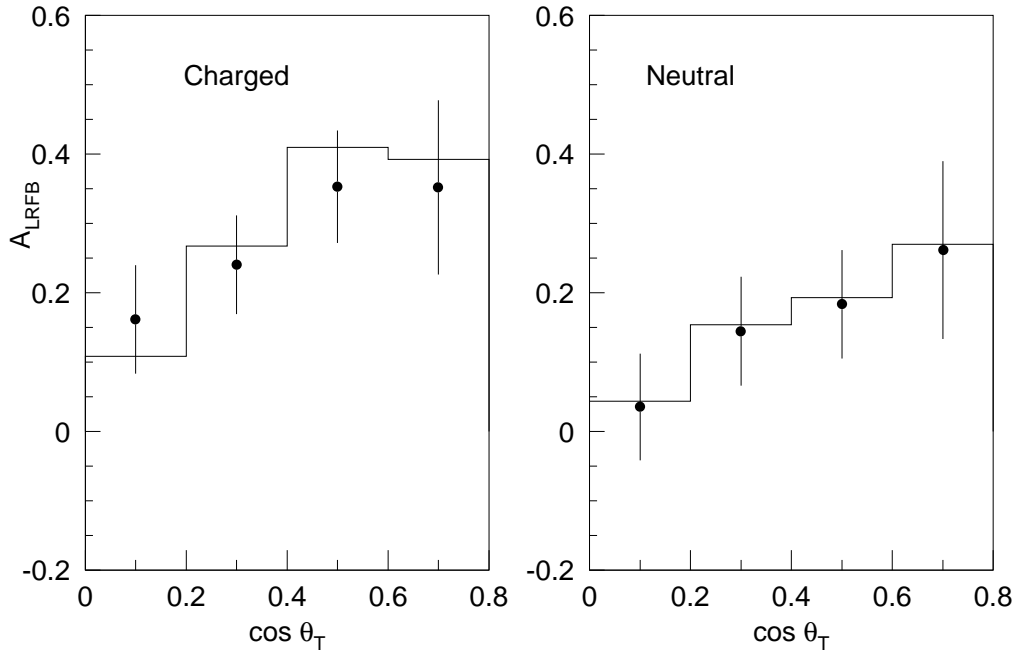


Figure 2: Left-right forward-backward asymmetry for charged and neutral vertices for data (points) and Monte Carlo simulation (histograms).

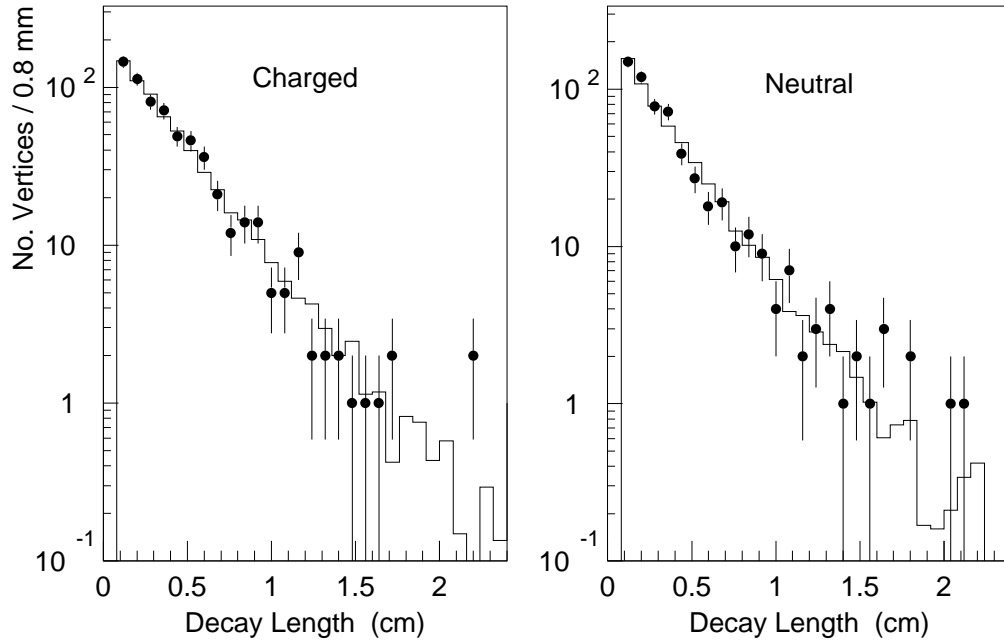


Figure 3: Decay length distributions for charged and neutral decays for data (points) and Monte Carlo simulation corresponding to the best fit (histograms).